Crystal Structure of the Complex of Bovine Pancreatic Phospholipase A_2 with the Inhibitor 1-Hexadecyl-3-(trifluoroethyl)-*sn*-glycero-2-phosphomethanol[†,‡]

Kanagaraj Sekar,[§] Subramaniam Eswaramoorthy,[§] Mahendra K. Jain,[||] and Muttaiya Sundaralingam*[,§]

Biological Macromolecular Structure Center, Departments of Chemistry and Biochemistry, and The Ohio State Biochemistry Program, 100 West 18th Avenue, The Ohio State University, Columbus, Ohio 43210, and Departments of Chemistry and Biochemistry, University of Delaware, Newark, Delaware 19716

Received June 9, 1997; Revised Manuscript Received September 15, 1997[⊗]

ABSTRACT: The structure of recombinant bovine pancreatic phospholipase A_2 (PLA2) complexed with the competitive inhibitor 1-hexadecyl-3-(trifluoroethyl)-*sn*-glycero -2-phosphomethanol (hereafter MJ33), a phospholipid analogue without the *sn*-3 phosphodiester group, has been determined. The crystals are trigonal, space group $P3_121$, $a = b = 46.36$ Å and $c = 102.56$ Å, and isomorphous to the recombinant PLA2 with one molecule in the asymmetric unit. The structure was refined using 8082 reflections between 8.0 and 1.91 Å resolution to a final *R*-value of 18.4% [$R_{free} = 28.0\%$]. The model includes 957 protein atoms, 86 water molecules, one calcium ion, and 26 non-hydrogen atoms of the inhibitor MJ33. The overall tertiary fold of the complex is very similar to that of the inhibitor-free recombinant PLA2 with a root mean square deviation of 0.32 Å for all the backbone atoms. The electron density of the surface loop residues 62−66 is clear and ordered, unlike the other trigonal bovine PLA2 structures done to date. This structural change could be responsible for the interfacial allosteric activation, which thermodynamically relates the enhanced binding of the substrate mimic to the active site of the enzyme. MJ33 is tightly bound in the active-site cleft, dislodging the equatorial coordinated calcium water (W5), the putative catalytic water W6, and the neighboring water W7. The axial coordinated calcium water is missing; thus the hexacoordinated calcium is a monocapped pentagonal pyramid. Although MJ33 is a *sn*-2 tetrahedral mimic, its phosphate binds to PLA2 differently from the *sn*-2 phosphonate analogue of phospholipids, another tetrahedral mimic. The knowledge of the active-site geometry of MJ33 would be useful in the design of more useful therapeutic agents for PLA2.

Secreted phospholipase A_2 (PLA2) specifically cleaves the *sn*-2 acyl ester bond of phospholipids. It has an absolute requirement for calcium as a cofactor for the substrate binding and for the chemical step of the catalytic cycle (Yu et al., 1993). Also, there is an absolute requirement for the *sn*-3 phosphodiester bond in the chemical step (Rogers et al., 1996). Several different classes of phospholipase A_2 have emerged in recent years; therefore, it is of interest to develop specific inhibitors for each class. Several crystal structures of the tetrahedral mimic inhibitor with an *sn*-2 phosphonate substituent, L-1-(*O*-octyl-2-(heptyl phosphonyl)-*sn*-glycero-3-phosphoethanolamine (TSA), complexed with secreted PLA2 from Chinese cobra venom (White et al., 1990), bee venom (Scott et al., 1990b), inflammatory exudate (Scott et al., 1991), and recombinant bovine pancreatic PLA2 (Sekar et al., 1997c) have been reported. Also the crystal structure of the *sn*-2 acyl amino analogue of phospholipid complexed with the engineered (without the residues of the surface loop 62−66) porcine PLA2 (Thunnissen et al., 1990) has been determined. Other crystal structures of interest include bovine pancreatic PLA2 with the inhibitor *n*-dodecylphosphorylcholine (Tomoo et al., 1994) and the human synovial PLA2 with an acyl amino analogue of phospholipids (Cha et al., 1996).

Potent competitive inhibitors with more significant changes in the glycerophospholipid structure have been reported (Jain et al., 1991b). For example, in MJ33 (Figure 1), the charged *sn*-3 phosphodiester group is replaced by a nonpolar short alkyl group and the *sn*-2 phosphodiester substituent is a tetrahedral mimic. This class of inhibitors are stable against acyl esterases as well as phospholipase A_1, C, and D, and therefore they are suited for in vivo studies where phospholipids may be more readily metabolized. For example, these inhibitors have provided insights into the biological role of PLA2 in surfactant production in lung (Fisher et al., 1992), platelet activation (Bartoli et al., 1994), permeability barrier homeostasis in skin (Man et al., 1996), esophagitis (Kim et al., 1997), and intestinal cholesterol uptake (Homan & Krause, 1997). To understand its mode of binding, we have cocrystallized the inhibitor MJ33 with PLA2. The refined structure of the complex shows that the *pro-S* oxygen of the *sn*-2 phosphate provides a ligand to the hexacoordinated calcium. Significant differences are also noted compared to other *sn*-2 tetrahedral mimics of phospholipids.

MATERIALS AND METHODS

Recombinant bovine pancreatic PLA2 was supplied by Dr. M.-D. Tsai. Crystals of the PLA2−MJ33 complex were obtained by cocrystallization, which grew over a period of 7 months. Crystallization was carried out by the hanging

[†] This work was supported by National Institutes of Health Grants GM 45947 (M.S.) and GM 29703 (M.K.J.) and an Ohio Regents Eminent Scholar endowment chair to M.S. We thank the Ohio Board of Regents Investment Fund for partial support toward the purchase of the R-axis IIc imaging plate X-ray data acquisition system.

[‡] The atomic coordinates and structure factors have been deposited with the Brookhaven Protein Data Bank with accession codes 1FDK and R1FDKSF, respectively.

* To whom correspondence should be addressed. Phone (614)-292-2925; Fax (614)-292-2524, E-mail sunda@biot.mps.ohio-state.edu.

[§] The Ohio State University.

[||] University of Delaware.

[⊗] Abstract published in *Advance ACS Abstracts,* November 1, 1997.

S0006-2960(97)01370-6 CCC: $14.00

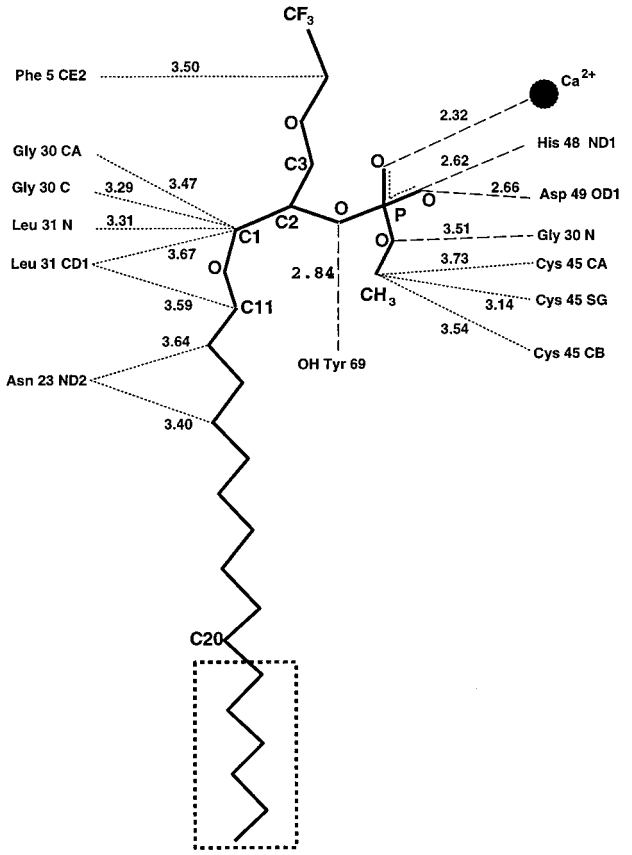

FIGURE 1: Schematic drawing of the inhibitor MJ33, 1-hexadecyl-3-(trifluoroethyl)-*sn*-glycero-2-phosphomethanol. The last six atoms of the *sn*-1 α-acyl chain (enclosed in the dotted box) are not visible in the electron density map. The hydrophobic interactions (≤3.8 Å) with the protein are shown with dotted lines. The hydrogen bonds and the calcium coordination are shown with dashed lines. The distances are in angstroms.

drop vapor diffusion method at room temperature (291 K) from a droplet containing 5 μL of the protein (15 mg/mL), 5 mM $CaCl_2$, 50 mM Tris buffer, pH 7.2, 2 μL of MPD (75%), and 1 μL of MJ33 inhibitor solution (2.5 mM concentration). The reservoir MPD concentration was 50%. The crystals were trigonal and isomorphous to those of the recombinant PLA2 (Sekar et al., 1997b). The space group is $P3_121$ and unit cell parameters are $a = b = 46.36$ Å and $c = 102.56$ Å with one molecule in the asymmetric unit. X-ray intensity data were collected from a crystal with dimensions 0.25 × 0.25 × 0.30 mm on our in-house R-axis IIc imaging plate system at room temperature (291 K). A total of 38 344 observations were measured to 1.91 Å resolution, which gave 8505 unique reflections [$F \geq 2\sigma(F)$]. The atomic coordinates of the trigonal form of the inhibitor-free recombinant PLA2 (PDB code 1MKT) were used as the starting model (Sekar et al., 1997b). A total of 5% of the reflections (423) were used to calculate the R_{free} (Brunger, 1992a) and the remaining 8082 reflections were used to carry out the refinement. Twenty-five cycles of rigid-body refinement with 8082 reflections between 8.0−1.91Å resolution gave an *R*-factor of 29.5% [$R_{free} = 33.0\%$] for only the 957 protein atoms. Further refinement by simulated annealing, employing a standard slow-cooling protocol, starting from 3000 K and cooling to 300 K with a temperature decrement of 25 K at 0.5 fs, then followed by 150 cycles of Powell minimization and 15 cycles of individual isotropic temperature factor, dropped the *R*-value to 23.4% [$R_{free} = 31.1\%$]. The difference electron density map clearly showed the calcium ion, the phosphate, and the trifluoroethyl groups of MJ33. Refinement of the positional and individual *B*-factors of these and 31 solvent molecules initially located lowered the *R*-factor to 21.5% [$R_{free} = 28.9\%$]. The resulting $|F_o| - |F_c|$ and $2|F_o| - |F_c|$ difference electron density maps clearly showed that most of the inhibitor MJ33, including the glycerol moiety, was in the active-site cleft. During the progress of the refinement, 55 additional solvent molecules were picked and included in the refinement. Only 26 atoms of the inhibitor out of 32 (Figure 1) were visible and fitted to the map. The 123 residues of the protein, the calcium ion, the 26 inhibitor atoms, and a total of 86 solvent molecules were subjected to a few more cycles of positional and individual isotropic *B*-factor refinement. Much of the lower extremities of the *sn*-1 α-acyl chain of MJ33 was still not visible in the omit electron density maps. Difference electron density maps and omit maps (omitting 10 residues at a time) were calculated and used to correct or rebuild parts of the model and the inhibitor by using the interactive molecular modeling program FRODO (Jones, 1985). The final refinement gave an *R*-value of 18.4% [$R_{free} = 28.0\%$] for 8082 reflections [$F \geq 2\sigma(F)$] in the resolution range 8.0−1.91 Å. All the above refinements were carried out using the XPLOR 3.1 program package (Brunger, 1992b) and the restraint parameters (Engh & Huber, 1991). The quality of the final model was assessed by using the program PROCHECK (Laskowski et al., 1993). The backbone dihedral angles for all the residues fall within the allowed regions of the Ramachandran plot. The coordinate error is estimated to be 0.2Å (Luzzatti, 1952). The main chain atoms of the inhibitor complex gave an RMS deviation of 0.32Å with the recombinant PLA2. The relevant refinement and stereochemical parameters for the final PLA2-MJ33 model are given in Table 1.

Table 1: Crystal Parameters and Other Relevant Geometric Parameters of the MJ33 Inhibitor Complex of PLA2

unit cell dimensions (Å)	$a = b = 46.36$, $c = 102.56$
space group	$P3_121$
resolution range (Å)	8.0−1.91
measured reflections	38 344
unique reflections	8505
R_{merge}[a] (%)	8.7
cumulative completeness (%) at 1.91 Å	83
R_{work} (8082 reflections) (%)	18.4
R_{free} (423 reflections) (%)	28.0
protein model	
protein atoms	957
water molecules	86
bound calcium ion (Ca^{2+})	1
inhibitor atoms	26
RMS deviation from ideal bond lengths (Å)	0.013
RMS deviation from ideal bond angles (deg)	1.53
RMS deviation from ideal dihedral (deg)	22.66
RMS deviation from ideal improper (deg)	1.21
average atomic temperature factors of the refined model (Å^2)	
main-chain atoms	23.2
side-chain atoms	26.9
water molecules	35.6
calcium ion	25.7
inhibitor atoms	44.6

[a] $R_{merge} = \sum_{hkl}|I - \langle I\rangle|/\sum I$, where *I* is the observed intensity and $\langle I\rangle$ is the average intensity from observations of symmetry related reflections respectively.

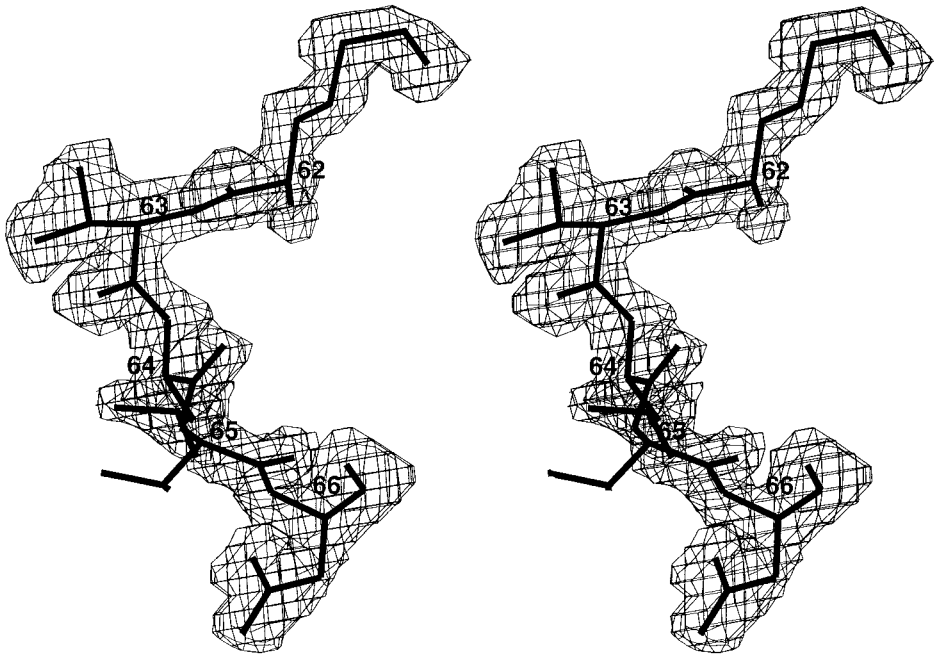

FIGURE 2: Stereoview of the omit electron density contoured at 0.8σ level for the ordered surface loop residues 62−66. The electron density is generally clear except for the side-chain atoms of Val 65.

RESULTS AND DISCUSSION

The 62−66 Surface Loop Is Ordered. For the first time in the trigonal crystal of PLA2, the main chain of the surface loop residues 62−66 is ordered and the electron density is clear (Figure 2). The only residue not visible in the electron density is Val 65, whose side chain beyond Cα is disordered. The 62−66 loop could influence the binding of the enzyme to the interface. The fact that binding of MJ33 makes it ordered may account for the observation that the occupancy of the active site of the enzyme in the aqueous phase increases by about 50-fold the affinity of the enzyme for the interface (Jain et al., 1993). Since the enhanced affinity is thermodynamically related to the allosteric effect of the interface on the substrate binding by the enzyme at the interface, ordering of the 62−66 loop could provide a structural basis for the K_s* allosteric interfacial activation of PLA2.

MJ33 Binds to the Active Site. The electron density is exceptionally clear for the inhibitor (Figure 4b), allowing a detailed description of the interactions. The bridging electron density for the atom C15 is not visible as shown in Figure 4b in the omit map at the contour level used (1.0σ) but was fitted using a lower contour level (0.6σ). The phosphate group is located between the essential calcium ion and the active-site residue His 48 (Figure 3a). The ordered part (C11−C20) of the long *sn*-1 α-acyl chain is stabilized by the hydrophobic interactions of the side-chain residues Leu 2, Asn 23, Asn 24, and Leu 31 (Figure 1). The last six atoms (C21−C26) are completely exposed to the bulk solvent and probably disordered. Note that the position of the *sn*-1 chain in MJ33 and TSA is almost the same (Figure 3) with close contacts with Gly 30, Leu 31, and Asn 23.

The glycerol backbone (C1-C2-C3) containing the trifluoroethyl group at C3 of MJ33, replacing the *sn*-3 phosphate of TSA, is rotated in the opposite direction (Figure 3b). In addition, the position of the *sn*-2 phosphate group of MJ33 is shifted by 0.76 Å compared to the *sn*-2 phosphonate group of the TSA (Figure 3b), and the phosphate anionic oxygen atoms of MJ33 are rotated by 53° clockwise relative to that of the phosphonate group (Figure 3c). This results in the movement of the C2 atom of the glycerol backbone in MJ33 downward (Figure 3c) by 3.35 Å, placing the terminal six atoms of the α-acyl chain (shown in dotted box, Figure 1) in the water channel and therefore disordered. Of course, in the interface the exposed part of the chain will be extended in the bilayer.

Four Water Molecules in the Active Site Are Replaced. In the bovine PLA2 structure, the coordination of calcium is a pentagonal bipyramid (Figure 4a). Besides the two calcium-coordinated water molecules (W5 and W12), there are two additional water molecules in the vicinity, the putative catalytic water W6 and a second water W7, which lie on either side of the His 48 plane and are hydrogen-bonded to Nδ1 of His 48 (Figure 4a). The catalytic water is further hydrogen-bonded to the equatorial calcium water, W5, thus connecting the catalytic dyad (His 48/Asp 99) to the calcium coordination sphere (Figure 4a). The other water molecule W7 to Nδ1 of His 48 is hydrogen-bonded to the carboxylate oxygen Oδ1 of Asp 49. These four water molecules (two calcium waters, W5 and W12, and the two histidine waters, W6 and W7) are intimately involved in the PLA2 active site. The "catalytic" water, W6, is believed to act as a nucleophile for enzymatic action and is presumably responsible for the cleavage of the *sn*-2 acyl ester bond of the phospholipid substrate (Dijkstra et al., 1981; Scott et al., 1990a). But later studies have utilized both the catalytic water W6 and the equatorial calcium coordinated water W5 in the mechanism of substrate hydrolysis (Rogers et al., 1996; Sekar et al., 1997a).

In all the earlier PLA2−inhibitor complexes, three water molecules (W5, W6, and W12) are replaced by the *sn*-2 and/or *sn*-3 substituents of the inhibitor. This replacement of water molecules in the active site by the isomorphic oxygens of the inhibitor has also been observed in earlier studies (Scott et al., 1990b, 1991; White et al., 1990; Thunnissen et al., 1990; Cha et al., 1996; Sekar et al., 1997c). The

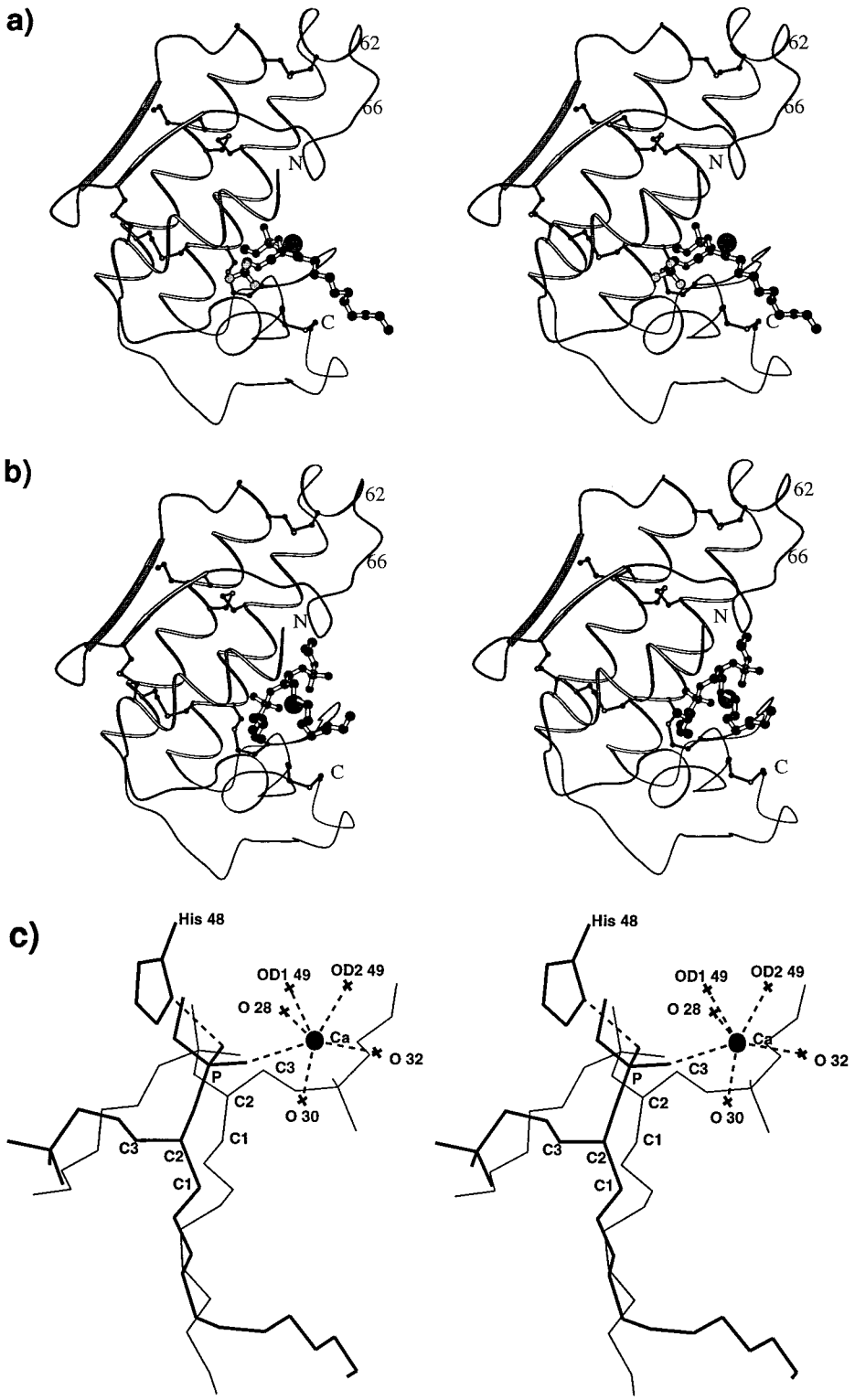

FIGURE 3: Stereoview of the ribbon diagram showing the active-site cleft and the bound inhibitors (a) MJ33 and (b) TSA and the seven disulfide bonds of the protein. The calcium ion is shown as a solid circle. (c) Stereoview of the superposition of the MJ33 complex (thick lines) with the TSA inhibitor (thin lines). The calcium ligands are shown. The phosphate atoms of MJ33 and TSA are 0.76 Å apart, while the glycerol C2 atom of MJ33 is lowered by 3.35 Å from that of TSA. Besides, the C3 atom of MJ33 is rotated on the opposite side to that of TSA. Panels a and b were produced using the program MOLSCRIPT (Kraulis, 1992).

exception is the inhibitor *n*-dodecylphosphorylcholine−PLA2 complex, where only W5 is substituted by the anionic oxygen atom of the phosphate group of the inhibitor (Tomoo et al., 1994) and no mention was made of the fate of other water molecules in the active site.

In the PLA2−MJ33 complex, the equatorial calcium-coordinated water molecule W5 is substituted by the anionic oxygen (*pro-S*) atom of the *sn*-2-phosphate group of MJ33 (Figure 4b) as in the other inhibitors. The other anionic oxygen (*pro-R*) atom comes in between the two histidine waters in the plane, displacing them and hydrogen-bonding to Nδ1 (Figure 4b). Thus these three active-site water molecules are displaced by the inhibitor. The axial calcium-coordinated water molecule is not visible in the electron density, resulting in the absence of all the four water molecules in the active site. It is clear from the above studies that the water ligation

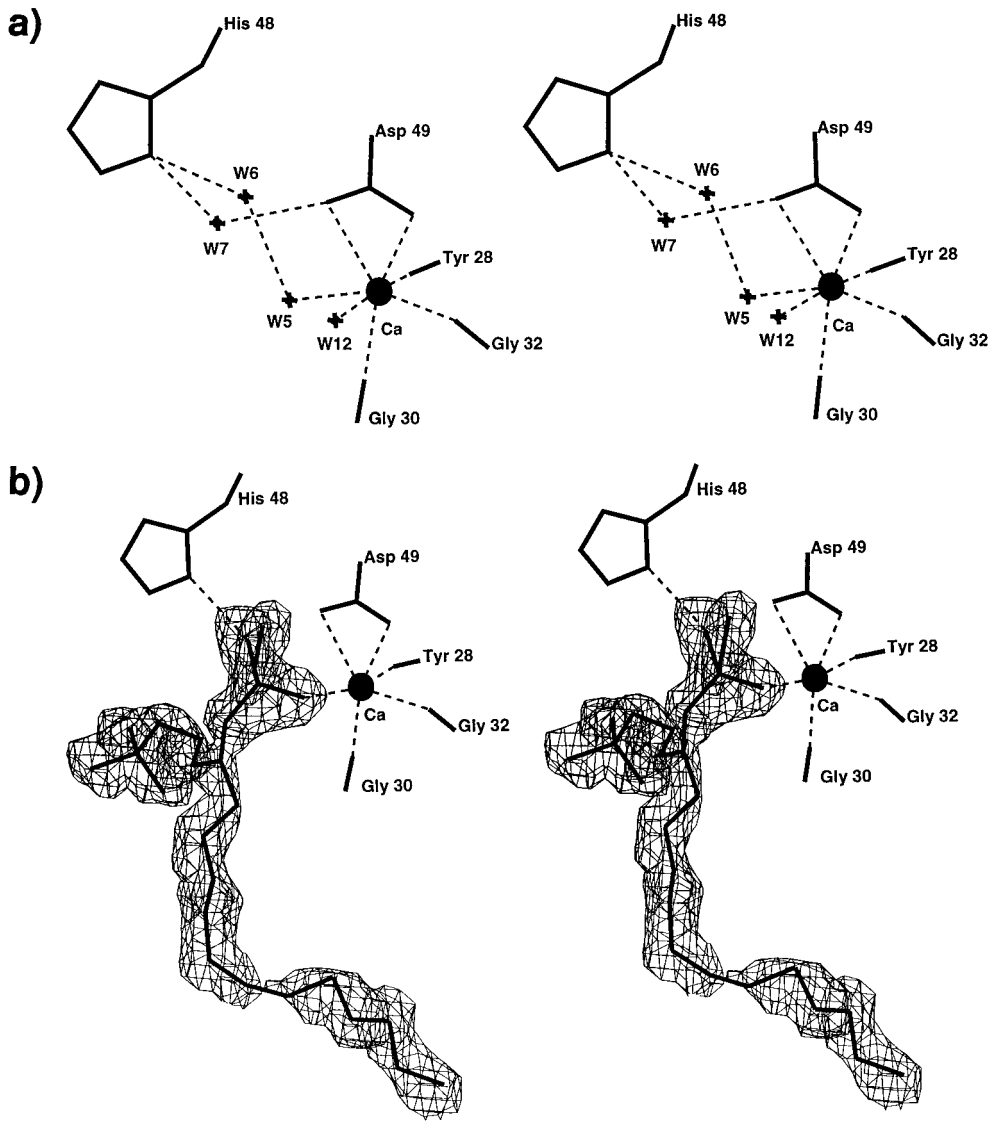

FIGURE 4: (a) Stereoview of the trigonal recombinant PLA2 calcium ion and its ligands in the pentagonal bipyramidal coordination. The water molecules W5 and W12 are involved in the calcium coordination, while W6 and W7 are hydrogen-bonded to the imidazole nitrogen Nδ1 of His 48. (b) Stereo plot showing the electron density of the inhibitor MJ33 and the calcium coordination. The equatorial calcium-coordinated water W5 is substituted by the *sn*-2 phosphate anionic oxygen (*pro-S*) atom and the second anionic oxygen (*pro-R*) atom lies between W6 and W7 and replaces them. The axial calcium-coordinated water W12 is missing.

to calcium is conserved (Ca···O═P) and the other substituents for W6 and W7 are flexible. The conserved structural water connected to Ala 1, stabilizing the active-site residues, is retained as in the earlier PLA2-inhibitor complexes (e.g., Scott et al., 1990a; Sekar et al., 1997c).

Calcium Is Hexacoordinated. In the PLA2−MJ33 complex, the axial calcium-coordinated water is missing, resulting in a monocapped pentagonal pyramid (six coordination, Figure 4b compared to the pentagonal bipyramid (seven coordination) in all other PLA2 structures (Figure 4a). The six calcium−ligand distances are between 2.19 and 2.69 Å with an average of 2.39 Å and were not constrained during the refinement. All the atoms of the residues involved in the calcium coordination (Tyr 28, Gly 30, Gly 32, and Asp 49) and the catalytic residue His 48 superpose well with the corresponding atoms of the trigonal form of the recombinant structure indicating virtually no perturbation in the active-site architecture. The side chain of Tyr 69 has swung out (Thunnissen et al., 1990; Scott et al., 1990b) and forms a hydrogen bond with the *sn*-2 ester oxygen atom.

Insights into Inhibition Kinetics. Having established the structure of MJ33 in the active site of PLA2 supports and provides insights into the kinetics of inhibition (Jain et al., 1991b). Although racemic MJ33 was used for crystallization, only *sn*-3 trifluoroethyl isomer was found in the cocrystal, in accord with its 50-fold higher affinity seen in the equilibrium binding and the kinetic studies. The crystal structure also confirms the key result of the protection method for the determination of interfacial equilibrium dissociation constants (Jain et al., 1991a), which showed that calcium is obligatory for the binding of MJ33 and other active-site-directed mimics (Yu et al., 1993). As an inhibitor, MJ33 is as effective as the *sn*-2 phosphonate or *sn*-2 amide analogues of phospholipids with the *sn*-3 phosphodiester group (Jain et al., 1991b). Thus, in conjunction with the crystallographic results it may be suggested that the *sn*-3 phosphate is not critical for the calcium-dependent binding of these mimics to the active site; however, the requirement for the *sn*-3 phosphate is absolute for the chemical step of the catalytic cycle (Rogers et al., 1996).

Kinetic and equilibrium binding results, expressed as interfacial dissociation constant in mole fraction units, showed that the octyl analogue of MJ33 is as effective an inhibitor of PLA2 as MJ33 with a hexadecyl chain. Of course, the effective inhibition expressed in terms of the bulk concentration is different because the partitioning of an inhibitor in the interface determines the mole fraction of the inhibitor that the enzyme "sees" in the interface (Jain et al., 1993). This conclusion is also supported by the crystallographic results, which show that the octyl and hexadecyl chains will make effectively the same contact. Also note that, during interfacial catalysis, the chain moves from the bilayer environment to a hydrophobic pocket of the enzyme, which supports the contention that the chain contacts contributes very little to the overall binding energy for the formation of the complex. Although the identity of the catalytic water is still uncertain (Seshadri et al., 1994; Rogers et al., 1996; and Sekar et al., 1997a), the crystallographic results are generally consistent with models that invoke a critical role for calcium and histidine in the binding of the substrate as well as in the rate-limiting chemical step of the catalytic cycle. Accommodation of a range of phospholipid head groups in the active site and the changes in the coordination environment of the calcium cofactor suggest that considerable conformational flexibility can be tolerated.

REFERENCES

Bartoli, F., Lin, H. K., Ghomashchi, F., Gelb, M. G., Jain, M. K., & Apitz-Castro, R. (1994) *J. Biol. Chem. 269*, 15625−15630.

Brunger, A. T. (1992a) *Nature 355*, 472−474.

Brunger, A. T. (1992b) *X-PLOR manual*, version 3.1, Yale University, New Haven, CT.

Cha, S.-S., Lee, D., Adams, J., Kurdyla, J. T., Jones, C. S., Marshall, L. A., Bolognese, B., Abdel-Meguid, S. S., & Oh, B.-H. (1996) *J. Med. Chem. 39*, 3878−3881.

Engh, R. A., & Huber, R. (1991) *Acta Crystallogr. A47*, 392−400.

Dijkstra, B. W., Drenth, J., & Kalk, K. H. (1981) *Nature 289*, 604−606.

Fisher, A. B., Dodia, C., Chander, A., & Jain, M. K. (1992) *Biochem. J. 288*, 407−411.

Homan, R., & Krause, B. R. (1997) *Curr. Pharm. Des. 3*, 29−44.

Jain, M. K., Ranadive, G. N., Rogers, J., Yu, B.-Z., & Berg, O. G. (1991a) *Biochemistry 30*, 7306−7317.

Jain, M. K., Tao, W., Rogers, J., Arenson, C., Eibl, H., & Yu, B.-Z. (1991b) *Biochemistry 30*, 10256−10268.

Jain, M. K., Yu, B.-Z., & Berg, O. G. (1993) *Biochemistry 32*, 11319−11329.

Jones, T. A. (1985) *Methods Enzymol. 115*, 157−171.

Kim, N., Sohn, V. D., Mangannan, V., Rich, H., Jain, M. K., Behar, J., & Biancani, P. (1997) *Gastroenterology 112*, 1548−1558.

Kraulis, P. J. (1992). *J. Appl. Crystallogr. 24*, 946−950.

Laskowski, R,A,, MacArthur, M. W., Moss, D. S., & Thornton, J. M. (1993) *J. Appl. Crystallogr. 26*, 283−291.

Luzzati, V. (1952) *Acta Crystallogr. 5*, 802−807.

Man, M. Q., Jain, M. K., Feingold, K. R., & Elias, P. M. (1996) *J. Invest. Dermatol. 106*, 57−63.

Rogers, J., Yu, B.-Z., Serves, S. V., Tsivgoulis, G. M., Sotiropoulos, D. N., Ioannou, P. V., & Jain, M. K. (1996) *Biochemistry 35*, 9375−9385.

Scott, D. L., White, S. P., Otwinowski, Z., Yuan, W., Gelb, M. H., & Sigler, P. B. (1990a) *Science 250*, 1541−1546.

Scott, D. L., Otwinowski, Z., Gelb, M. H., & Sigler, P. B. (1990b) *Science 250*, 1563−1566.

Scott, D. L., White, S. P., Browning, J. L., Rosa, J. J., Gelb, M. H., & Sigler, P. B. (1991) *Science 254*, 1007−1010.

Sekar, K., Yu, B.-Z., Rogers, J., Lutton, J., Liu, X., Chen, X., Tsai, M.-D., Jain, M. K., & Sundaralingam, M. (1997a) *Biochemistry 36*, 3104−3114.

Sekar, K., Sekharudu, C., Tsai, M.-D., & Sundaralingam, M. (1997b) (*Acta Crystallogr. D* (in press).

Sekar, K., Kumar, A., Liu, X., Tsai, M-D., Gelb, M. H., & Sundaralingam, M. (1997c) *Acta Crystallogr. D* (in press).

Seshadri, K., Vishveshwara, S., & Jain, M. K. (1994) *Proc. Ind. Acad. Sci. 106*, 1177−1189.

Thunnissen, M. M. G. M., Eiso, A. B., Kalk, K. H., Drenth, J., Dijkstra, B. W., Kuipers, O. P., Dijkman, R., de Hass, G. H., & Verheij, H. M. (1990) *Nature 347*, 689−691.

Tomoo, K., Ohishi, H., Ishida, T., Inoue, M., Ikeda, K., Sumiya, S., & Kitamura, K. (1994) *Proteins*: *Struct., Funct., Genet. 19*, 330−339.

White, S. P., Scott, D. L., Otwinowski, Z., Gelb, M. H., & Sigler, P. B. (1990) *Science 250*, 1560−1563.

Yu, B.-Z., Berg, O. G., & Jain, M. K. (1993) *Biochemistry 32*, 6485−6492.

Yuan, W., & Gelb, M. H. (1988) *J. Am. Chem. Soc. 110*, 2665−2666.

BI971370B